Table 1. Hook length of switch gene mutants in *S. enterica* serovar Typhimurium. The phenotypes of Che⁻ mutants were either tumbled (T) or smooth (S) swimming. The mutation sites were taken from (*25*) and (*26*); amino acid abbreviations are given in (*27*). The hook length data show the average hook length ± SD. The total number of measured particles is indicated in parentheses. n.d., not determined; dash indicates that only a few examples were observed (see Fig. 1C).

Gene	Phenotype	Strain number	Mutation sites	Hook length (nm)
fliG	Che⁻ (T)	SJW2323	V135F	26.4 ± 6.9 (101)
	Che⁻ (S)	SJW2325	V135L	26.8 ± 8.0 (110)
	Mot⁻	SJW2834	R160H	44.0 ± 7.0 (110)
	Che⁻ (T)	SJW2332	G185D	43.1 ± 8.7 (110)
	Mot⁻	SJW2826	Δ282–287	28.5 ± 6.7 (111)
fliM	Che⁻ (T)	SJW2308	E59K	24.1 ± 7.4 (70)
	Che⁻ (T)	SJW2299	R60C	24.7 ± 6.4 (104)
	Che⁻ (T)	SJW2309	R63C	25.9 ± 6.2 (71)
	Mot⁻	SJW1813	H106P	41.8 ± 6.8 (109)
	Mot⁻	SJW1764	F131C	45.7 ± 3.7 (109)
	Mot⁻	SJW1806	G133D	45.1 ± 5.1 (114)
	Che⁻ (S)	SJW2293	G143C	23.3 ± 6.0 (123)
	Mot⁻	SJW1814	T147I	28.1 ± 7.6 (123)
	Che⁻ (T)	SJW2312*	R181C	24.6 ± 7.3 (121)
	Che⁻ (T)	SJW2311*	R181S	26.8 ± 6.7 (57)
	Che⁻ (T)	SJW2310*	R181L	27.1 ± 8.4 (33)
	Mot⁻	SJW1804	L250Q	26.5 ± 6.1 (110)
fliN	Che⁻ (S)	SJW2287	G94S	23.4 ± 7.2 (62)
	Mot⁻	SJW1765	L105Q	27.1 ± 7.0 (117)
	Mot⁻	SJW1784	n.d.	47.0 ± 6.9 (148)
	Mot⁻	SJW1809	n.d.	44.4 ± 6.3 (109)
	Mot⁻	SJW1810	n.d.	46.2 ± 5.1 (93)
fliM	Fla⁻	SJW2409	n.d.	—

*These mutants were derived from SJW806, whereas the others were from SJW1103 (*9*).

determine the hook length, and the C ring may act as a quantized measuring cup. The unit capacity and the subsequent unit hook length would be 30 subunits and 14 nm, as found in SJW2409 (*fliM* /Fla⁻) (Fig. 1C).

If FliK is not a molecular ruler of hook length, then what is the role of FliK? The length distribution of polyhooks shows a peak at 55 nm, indicating that the hook length is controlled, even in the absence of FliK (*21*). In order to terminate the elongation, the hook-cap protein (FlgD) has to be replaced by a hook-filament junction protein (FlgK). However, FlgK itself is not necessary for the hook length control (*3*). In most *fliK* mutants, FlgD stays at the tip of the hook, allowing the continuous elongation of the hook (*22*). The flagellar secretion system has two modes: one specific for the hook proteins and the other for flagellin (*23*). These *flgK* mutants secrete large amounts of flagellin into media, indicating that the secretion mode is turned to the latter (*24*). Moreover, the *flgK* mutants secrete FliK, which terminates the secretion of hook proteins (*7*). Thus, FliK is likely to be required in the termination of hook elongation by changing the mode of secretion.

Thus, a mechanism of the hook length determination could be as follows. The hook monomers (FlgE) accumulate to fill the C ring and are secreted en bloc to form the hook of a finite length. When the C ring is empty, FliK is secreted, which converts the mode of secretion into that for flagellin. Then, FlgD at the tip of a nascent hook is replaced by FlgK, which terminates the hook elongation.

References and Notes

1. R. M. Macnab, in Escherichia coli *and* Salmonella typhimurium*: Cellular and Molecular Biology*, F. C. Neidhardt *et al.*, Eds. (American Society for Microbiology, Washington, DC, 1996), pp. 123–145.
2. S.-I. Aizawa, *Mol. Microbiol.* **19**, 1 (1996).
3. T. Hirano, S. Yamaguchi, K. Oosawa, S.-I. Aizawa, *J. Bacteriol.* **176**, 5439 (1994).
4. K. Kutsukake, *J. Bacteriol.* **179**, 1268 (1997).
5. K. Muramoto, S. Makishima, S.-I. Aizawa, R. M. Macnab, *J. Mol. Biol.* **277**, 871 (1998).
6. ———, *J. Bacteriol.* **181**, 5808 (1999).
7. T. Minamino, B. Gonzalez-Pedrajo, K. Yamaguchi, S.-I. Aizawa, R. M. Macnab, *Mol. Microbiol.* **34**, 295 (1999).
8. A. W. Williams *et al.*, *J. Bacteriol.* **178**, 2960 (1996).
9. S. Yamaguchi, H. Fujita, A. Ishihara, S.-I. Aizawa, R. M. Macnab, *J. Bacteriol.* **166**, 187 (1986).
10. S. Yamaguchi *et al.*, *J. Bacteriol.* **168**, 1172 (1986).
11. C. J. Hueck, *Microbiol. Mol. Biol. Rev.* **62**, 379 (1998).
12. T. Kubori *et al.*, *Science* **280**, 602 (1998).
13. T. Kubori, A. Aukhan, S.-I. Aizawa, J. E. Galan, *Proc. Natl. Acad. Sci. U.S.A.* **97**, 10225 (2000).
14. K. Tamano *et al.*, *EMBO J.* **19**, 3876 (2000).
15. S. A. Lloyd, F. G. Whitby, D. F. Blair, C. Hill, *Nature* **400**, 472 (1999).
16. T. Kubori, N. Shimamoto, S. Yamaguchi, K. Namba, S.-I. Aizawa, *J. Mol. Biol.* **226**, 433 (1992).
17. E. Katayama, T. Shiraishi, K. Oosawa, N. Baba, S.-I. Aizawa, *J. Mol. Biol.* **255**, 458 (1996).
18. I. H. Khan, T. S. Reese, S. Khan, *Proc. Natl. Acad. Sci. U.S.A.* **89**, 5956 (1992).
19. N. R. Francis, G. E. Sosinsky, D. Thomas, D. J. DeRosier, *J. Mol. Biol.* **235**, 1261 (1994).
20. C. J. Jones, R. M. Macnab, H. Okino, S.-I. Aizawa, *J. Mol. Biol.* **212**, 377 (1990).
21. S. Koroyasu, M. Yamazato, T. Hirano, S.-I. Aizawa, *Biophys. J.* **74**, 436 (1998).
22. K. Ohnishi *et al.*, *J. Bacteriol.* **176**, 2272 (1994).
23. T. Minamino, R. M. Macnab, *J. Bacteriol.* **181**, 1388 (1999).
24. K. Komoriya *et al.*, *Mol. Microbiol.* **34**, 767 (1999).
25. H. Sockett *et al.*, *J. Bacteriol.* **174**, 793 (1992).
26. V. M. Irikura *et al.*, *J. Bacteriol.* **175**, 802 (1993).
27. Single-letter abbreviations for the amino acid residues are as follows: C, Cys; D, Asp; E, Glu; F, Phe; G, Gly; H, His; I, Ile; K, Lys; L, Leu; P, Pro; Q, Gln; R, Arg; S, Ser; T, Thr; and V, Val.
28. We thank R. E. Sockett for polishing the English and T. Goto and S. Ishii for figures. This work was partially supported by Grant-in-Aid for Scientific Research (B) from The Ministry of Education, Science, Sports and Culture (Japan).

Preferential Localization of Effector Memory Cells in Nonlymphoid Tissue

David Masopust, Vaiva Vezys, Amanda L. Marzo, Leo Lefrançois*

Many intracellular pathogens infect a broad range of host tissues, but the importance of T cells for immunity in these sites is unclear because most of our understanding of antimicrobial T cell responses comes from analyses of lymphoid tissue. Here, we show that in response to viral or bacterial infection, antigen-specific CD8 T cells migrated to nonlymphoid tissues and were present as long-lived memory cells. Strikingly, CD8 memory T cells isolated from nonlymphoid tissues exhibited effector levels of lytic activity directly ex vivo, in contrast to their splenic counterparts. These results point to the existence of a population of extralymphoid effector memory T cells poised for immediate response to infection.

After encounter with antigen, CD8 T cells differentiate into effector cells, which form a crucial arm of the adaptive immune response against intracellular pathogens through the action of cytokines and cell-mediated cyto- toxicity (*1, 2*). Activation leads to proliferation and a large increase in antigen-specific cytotoxic T lymphocytes (CTLs); this effector population contracts after resolution of the infection, leading to a stable memory popu-

Fig. 1. Infection with VSV leads to the appearance of virus-specific CD8 T cells in lymphoid and nonlymphoid tissues. C57Bl/6J mice were infected intravenously with 10^6 plaque-forming units (PFU) of VSV-Indiana, and 8 days (**A**) or 81 days (**B**) later, mice were perfused and lymphocytes were isolated from the indicated tissues. The percentage of antigen-specific CD8 T cells was assessed by staining with N_{52-59}/K^b tetramer and antibodies to CD8α and CD11a, followed by fluorescence flow cytometry. Plots shown are gated on CD8α$^+$ lymphocytes; values are mean percentages of tetramer$^+$ cells within the CD8$^+$ T cell population derived from at least four mice. Control staining with a K^b tetramer containing SIINFEKL was negligible. PLN, peripheral lymph nodes; MLN, mesenteric lymph nodes; PBL, peripheral blood lymphocytes; LP, small intestine lamina propria; IEL, small intestine intraepithelial lymphocytes; BM, bone marrow; Perit, peritoneal cavity lymphocytes.
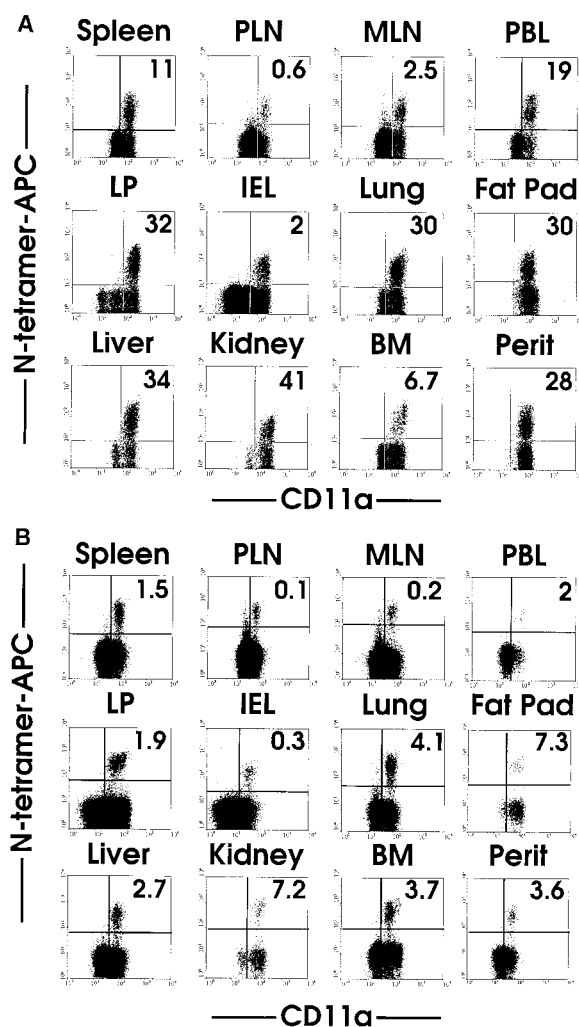

Table 1. Induction of peripheral tissue memory by *Listeria* or VSV infection. C57Bl/6J mice were infected by gavage with 10^9 colony-forming units of LM-ova or by intravenous injection with 10^6 plaque-forming units of VSV, and lymphocytes were isolated from numerous tissues at the indicated time points; the percentage of antigen-specific CD8 T cells was assessed by staining with SIINFEKL/K^b tetramer (LM-ova) or N_{52-59} tetramer (VSV) and antibodies to CD8α and CD11a, followed by fluorescence flow cytometry. Control staining with the irrelevant tetramer was negligible. Values represent the mean percentage of tetramer$^+$ cells of the CD8$^+$ T cell population $\pm$ standard error from three to six mice per time point. PLN, peripheral lymph node; MLN, mesenteric lymph node; PP, Peyer's patch; PBL, peripheral blood lymphocytes; BM, bone marrow; LP, small intestine lamina propria; IEL, small intestine intraepithelial lymphocytes; Perit, peritoneal lavage; ND, not detectable.

Tissue	LM-ova			VSV	
	Day 9	Day 20	Day 59	Day 81	Day 296
Spleen	5.51 ± 0.30	0.76 ± 0.15	0.38 ± 0.06	1.54 ± 0.33	1.24 ± 0.12
PLN	0.07 ± 0.02	ND	ND	0.14 ± 0.03	*
MLN	0.31 ± 0.03	ND	ND	0.18 ± 0.04	0.36 ± 0.02
PP	4.15 ± 0.92	0.52 ± 0.16	0.15 ± 0.04	*	ND
PBL	25.89 ± 3.42	2.69 ± 0.86	0.70 ± 0.06	2.09 ± 0.59	1.21 ± 0.09
BM	7.65 ± 0.67	*	1.49 ± 0.23	3.72 ± 0.52	2.61 ± 0.31
Lung	29.98 ± 1.81	6.36 ± 1.72	1.77 ± 0.12	4.06 ± 0.46	1.45 ± 0.19
LP	30.58 ± 3.98	12.38 ± 2.80	3.38 ± 0.68	1.86 ± 0.28	2.20 ± 0.12
IEL	3.46 ± 1.08	0.77 ± 0.38	0.20 ± 0.07	0.33 ± 0.15	0.21 ± 0.02
Liver	22.96 ± 1.34	3.64 ± 0.18	0.91 ± 0.09	2.88 ± 0.05	1.58 ± 0.40
Kidney	36.14 ± 3.01	21.56 ± 2.71	5.12 ± 0.29	7.20 ± 2.07	3.27 ± 1.76
Fat pad	39.43 ± 0.48	18.02 ± 2.75	6.47 ± 0.37	7.35 ± 0.27	4.03 ± 0.83
Perit	30.33 ± 3.41	11.37 ± 1.26	3.83 ± 1.68	3.57 ± 0.91	2.17 ± 0.72

*Not measured.

lation of intermediate frequency (*3–9*). Although CD8 memory cells are identifiable within secondary lymphoid organs (*4, 7, 10, 11*), their pattern of migration and their relationship with memory populations in other tissues remains unclear. Previous work demonstrated that T cells with a memory phenotype migrate through peripheral tissues, such as skin and intestine; hence, subsets of memory cells with a migratory preference for a given tissue may exist (*9, 12–14*). Recent data also indicate that human memory-phenotype CD4 and CD8 T lymphocytes within the blood may be divisible into two subsets on the basis of chemokine receptor expression and effector function (*15*). Although this theory is intriguing, the population dynamics and the functional status of pathogen-specific memory T cells within different tissues in vivo remain poorly characterized. Moreover, it is unknown whether memory T lymphocyte characteristics measured in lymphoid tissue are indicative of the overall memory population. To address these questions, we compared antigen-specific effector and memory CD8 T cells in lymphoid and nonlymphoid tissues after viral or bacterial infections.

C57Bl/6J mice were infected intravenously with vesicular stomatitis virus (VSV), Indiana serotype. Infection of mice with VSV is transient (*16*) and has been used as a model of a nonpersistent pathogen (*17, 18*). At various times after infection, we isolated lymphocytes from lymphoid and nonlymphoid tissues; we then used major histocompatibility complex (MHC) class I tetramers containing the immunodominant peptide epitope from the VSV nucleoprotein and H-2K^b (VSV-N_{52-59}/K^b) (*19*). MHC class I tetramers containing the appropriate antigenic peptide allow identification of antigen-specific CD8 T cells within an entire lymphocyte population (*6, 7, 20, 21*). Eight days after infection, VSV-specific CD8 T cells were present in all tissues examined, including spleen, peripheral and mesenteric lymph nodes, peripheral blood, small intestine lamina propria (LP) and intraepithelial lymphocyte (IEL) compartments, lung, fat pad, liver, kidney, bone marrow, and peritoneal cavity (Fig. 1A). Tetramer$^+$ cells in all tissues expressed high levels of CD11a, which is up-regulated by activation (Fig. 1A) and remains high on memory CD8 T cells (*22*). As a percentage of CD8 T cells, tetramer$^+$ cells were more prominent in nonlymphoid tissues than in secondary lymphoid tissues. To determine whether this phenomenon was unique to VSV infection, we infected mice orally with recombinant *Listeria*

Division of Immunology, Department of Medicine, University of Connecticut Health Center, Farmington, CT 06030, USA.

*To whom correspondence should be addressed. E-mail: llefranc@neuron.uchc.edu

monocytogenes expressing ovalbumin (LM-ova) (*23*) and visualized the response using H-2K^b/SIINFEKL tetramers (where SIIN-FEKL is the ova peptide, Ser-Ile-Ile-Asn-Phe-Glu-Lys-Leu). This infection resulted in generation of a robust anti-ova CD8 T cell response in all tissues (Table 1), in which high percentages of tetramer$^+$ cells were present in nonlymphoid sites. These data implied that migration of activated CD8 T cells to multiple tissues was independent of the infectious agent and the infection route.

To test whether localization of memory CD8 T cells reflected the primary response, we analyzed tissues at protracted times after infection. At 81 and 296 days after VSV infection, or at 20 and 59 days after *Listeria* infection, memory cells were detectable in all nonlymphoid tissues (Fig. 1B and Table 1). Differences were observed when the kinetics of the tissue responses were compared (Fig. 2A). Although the percentage of tetramer$^+$ cells in the spleen, lymph nodes, and blood declined rapidly, the response was prolonged in most other tissues. This finding, and the fact that tissues such as lung, liver, and kidney were perfused before lymphocyte isolation, indicated that the tetramer$^+$ cells detected were not derived from blood contamination. Interestingly, only very small populations of memory cells were present in lymph nodes, indicating a preference for CD8 memory cells to migrate and expand elsewhere. Among nonlymphoid tissues analyzed, the lung, liver, and small intestine LP contributed the majority of tetramer$^+$ cells. When total numbers of antigen-specific T cells per tissue were compared, the cumulative sum of the cell numbers in the lung, liver, and LP was similar to that in the spleen at the peak of the response, as the response declined, and in the memory phase of the response (Fig. 2B). Thus, the number of cells within nonlymphoid tissues represents a substantial portion of the overall response. The kinetics of the response with regard to total cell numbers in each tissue was distinct and did not always reflect the kinetics as calculated from percentages of tetramer$^+$ cells (Fig. 2B). Thus, relative to the spleen, tetramer$^+$ cell numbers in the LP and lung declined gradually while tetramer$^+$ cells in the liver declined rapidly. Nevertheless, a stable population of memory CD8 T cells was detectable in each tissue.

The distinct response kinetics observed in lymphoid versus nonlymphoid tissues prompted us to examine possible functional differences that might exist between the antigen-specific cells in different locations. Twenty days after VSV infection, short-term culture of cells with the N$_{52-59}$ peptide induced the majority of antigen-specific cells from all

tissues tested to produce interferon-γ (IFN-γ), based on percentages of tetramer$^+$ cells (Fig. 3A). Although in some cases the percentage of LP and lung cells responding was less than that observed by tetramer staining, this was not a consistent finding. However, when direct ex vivo antigen-specific lytic assays were performed, striking differences were observed between cells from lymphoid versus nonlymphoid sites. Twenty days after infection with VSV, high lytic activity was mediated by cells from LP, lung, and liver, but not by splenocytes at identical effector-to-target (E:T) ratios (Fig. 3B). At later times after infection, insufficient percentages of tetramer$^+$ cells were present in some tissues to allow a definitive comparison at overlapping E:T ratios. To circumvent this problem, we infected mice with VSV–New Jersey, a second VSV serotype that induces cross-reactive CTLs (*24, 25*), followed by secondary infection 7 months later with VSV-Indiana. This resulted in the generation of a larger VSV-specific memory population. Seven months after secondary infection, lymphocytes were assayed for ex vivo antigen-specific lytic activity. In agreement with previous reports, memory splenocytes exhibited low levels of

lytic activity (*4, 9, 26*). Lymphoid memory cells were, however, able to rapidly up-regulate lytic activity after antigen challenge (*9, 27*). Nevertheless, at comparable E:T ratios, CD8 T cells from liver, lung, and LP exhibited potent lytic activity (Fig. 3C). Experiments performed at 111 days (*28*) and 134 days (*27*) after secondary infection yielded similar results and also showed that the cell isolation procedures were not responsible for induction of lytic activity (*28*). Also, *Listeria*-specific memory cells in tertiary tissues were highly lytic (*27*).

We directly compared the lytic activity of primary anti-VSV effectors and memory T cells from spleen and lung. The lytic activity of primary splenic and lung effectors and of lung memory cells was comparable, whereas memory splenocytes had low activity (Fig. 3D). Therefore, migration through multiple nonlymphoid tissues was a hallmark of CD8 effector memory T cells generated through viral or bacterial infection. We also examined the size and phenotype of lymphoid and nonlymphoid memory cells (*28*). Although memory cells from all tissues were similar in size to naïve cells, phenotypic differences were noted between memory cells in the LP and other tissues, indicating that an intestinal mu-

Fig. 2. Tissue-specific kinetics of the anti-VSV CD8 T cell response. At the indicated numbers of days after infection, lymphocytes from four to eight mice were isolated and stained with tetramer and antibodies to CD8α and CD11a, then analyzed by fluorescence flow cytometry. At all time points, the total number of viable lymphocytes isolated per tissue was enumerated by trypan blue exclusion and light microscopy. (**A**) Kinetics of the response based on percentage of CD8$^+$ cells that were tetramer$^+$. Symbols: solid squares, spleen; right-pointing arrowheads, liver; left-pointing arrowheads, lung; triangles, kidney; inverted triangles, peritoneum; stars, PBL; open circles, PLN; solid circles, LP; diamonds, fat pad. (**B**) Kinetics of the response based on total numbers of tetramer$^+$ cells per tissue. Values were derived by multiplying the percentage of total lymphocytes that were tetramer$^+$ by the total number of lymphocytes isolated from that tissue. Values for "tissues" in the upper left panel (solid circles) were the total tetramer$^+$ cells from lung, liver, and LP. Values represent means ± standard error.
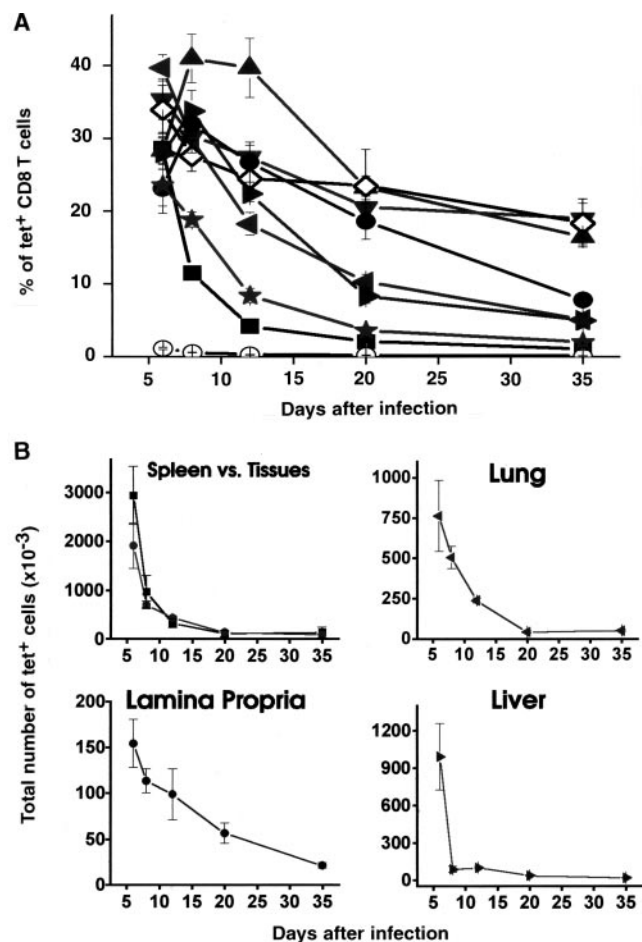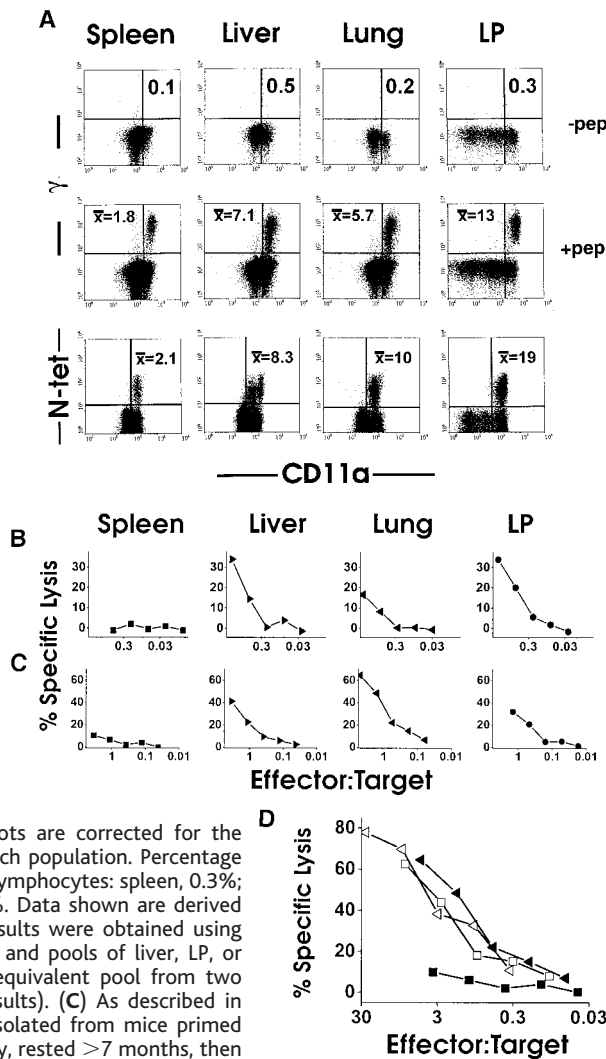
cosa-specific memory population may exist (*28*), as we previously suggested (*29*).

This study demonstrated that bacterial or viral infection resulted in margination of CD8 T cell effectors and memory cells into nonlymphoid tissues. Our results suggest that memory cells either continuously recirculate through peripheral tissues, or permanently reside in them. Previous studies have demonstrated the existence of activated as well as memory phenotype T cells in a limited number of tissues after a variety of infections (*6, 9, 30–32*), but the extent of CD8 T cell migration or retention during primary and memory phases of the response was not fully appreciated. Perhaps more important, our results demonstrate a functional distinction between tissue-homing or resident

memory cells and memory cells located in the secondary lymphoid organs. A previous study suggested that CCR7+CD62L+ central memory cells without immediate effector ability traffic through secondary lymphoid tissue, whereas CCR7−CD62L− effector memory T cells circulate outside of lymphoid tissue (*15*). Our data support the existence of functionally distinct memory T cell subsets, but also suggest additional complexity in the system, because CD62L− splenic and tissue memory cells had distinct functional abilities. We also cannot rule out the potential effects of persisting antigen on nonlymphoid memory cells, although antigen is not believed to be required for anti-LCMV (lymphocytic choriomeningitis virus) splenic CD8 memory cell survival (*33*). It will be im-

portant to determine whether memory cells undergo tissue-specific regulation and perhaps can be distinguished by the expression of distinct sets of homing molecules and chemokine receptors. Teleologically, the ability of memory cells in tertiary sites to exert immediate cytolytic activity provides a mechanism for improved survival of the organism via rapid containment of pathogens.

References and Notes

1. D. Kagi, B. Ledermann, K. Burki, R. M. Zinkernagel, H. Hengartner, *Annu. Rev. Immunol.* **14**, 207 (1996).
2. J. T. Harty, A. R. Tvinnereim, D. W. White, *Annu. Rev. Immunol.* **18**, 275 (2000).
3. R. Dobber, A. Hertogh-Huijbregts, J. Rozing, K. Bottomly, L. Nagelkerken, *Dev. Immunol.* **2**, 141 (1992).
4. C. Zimmermann, K. Brduscha-Riem, C. Blaser, R. M. Zinkernagel, H. Pircher, *J. Exp. Med.* **183**, 1367 (1996).
5. E. A. Butz, M. J. Bevan, *Immunity* **8**, 167 (1998).
6. K. J. Flynn *et al.*, *Immunity* **8**, 683 (1998).
7. K. Murali-Krishna *et al.*, *Immunity* **8**, 177 (1998).
8. D. H. Busch, I. M. Pilip, S. Vijh, E. G. Pamer, *Immunity* **8**, 353 (1998).
9. S. K. Kim, K. S. Schluns, L. Lefrançois, *J. Immunol.* **163**, 4125 (1999).
10. L. Bruno, J. Kirberg, H. von Boehmer, *Immunity* **2**, 37 (1995).
11. D. H. Busch, I. Pilip, E. G. Pamer, *J. Exp. Med.* **188**, 61 (1998).
12. E. C. Butcher, L. J. Picker, *Science* **272**, 60 (1996).
13. R. W. Dutton, L. M. Bradley, S. L. Swain, *Annu. Rev. Immunol.* **16**, 201 (1998).
14. U. H. von Andrian, C. R. Mackay, *N. Engl. J. Med.* **343**, 1020 (2000).
15. F. Sallusto, D. Lenig, R. Forster, M. Lipp, A. Lanzavecchia, *Nature* **401**, 708 (1999).
16. R. R. Wagner, *The Rhabdoviruses* (Plenum, New York, 1987).
17. T. M. Kundig *et al.*, *Immunol. Rev.* **150**, 63 (1996).
18. T. M. Kundig *et al.*, *Proc. Natl. Acad. Sci. U.S.A.* **93**, 9716 (1996).
19. G. M. Van Bleek, S. G. Nathenson, *Nature* **348**, 213 (1990).
20. J. D. Altman *et al.*, *Science* **274**, 94 (1996).
21. For production of MHC class I tetramers, bacteria-produced H-2K^b containing the BirA-dependent biotinylation substrate sequence was folded in the presence of human β2-microglobulin and the VSV-N peptide. Biotinylation was performed with biotin-protein ligase (Avidity, Denver, CO). Tetramers were then produced from biotinylated, high-performance liquid chromatography–purified monomers by addition of streptavidin-allophycocyanin (APC; Molecular Probes, Eugene, OR).
22. B. K. Cho, C. Wang, S. Sugawa, H. N. Eisen, J. Chen, *Proc. Natl. Acad. Sci. U.S.A.* **96**, 2976 (1999).
23. C. Pope *et al.*, *J. Immunol.* **166**, 3402 (2001).
24. L. Puddington, M. J. Bevan, J. K. Rose, L. Lefrançois, *J. Virol.* **60**, 708 (1986).
25. J. W. Yewdell *et al.*, *J. Exp. Med.* **163**, 1529 (1986).
26. L. K. Selin, R. M. Welsh, *J. Immunol.* **158**, 5366 (1997).
27. D. Masopust, L. Lefrançois, unpublished data.
28. Supplementary data are available at *Science* Online (www.sciencemag.org/cgi/content/full/291/5512/2413/DC1).
29. D. Masopust, J. Jiang, H. Shen, L. Lefrançois, *J. Immunol.* **166**, 2348 (2001).
30. M. K. Slifka, J. K. Whitmire, R. Ahmed, *Blood* **90**, 2103 (1997).
31. G. T. Belz, J. D. Altman, P. C. Doherty, *Proc. Natl. Acad. Sci. U.S.A.* **95**, 13812 (1998).
32. E. J. Usherwood *et al.*, *J. Virol.* **73**, 7278 (1999).
33. K. Murali-Krishna *et al.*, *Science* **286**, 1377 (1999).
34. Before tissue removal, mice were perfused with phosphate-buffered saline and heparin (75 U/ml). IEL and LP cells were isolated as described (*9*). Lung tissue was minced and incubated with stirring at 37°C for 30 min in Hanks' balanced salt solution (HBSS) with 1.3 mM EDTA, followed by treatment at 37°C for 1 hour with collagenase (150 U/ml;

Fig. 3. Virus-specific CD8 memory T cells in peripheral but not lymphoid tissues are constitutively cytolytic. (**A**) Twenty days after VSV infection, lymphocytes were isolated as described (*9, 34*) from spleen, liver, lung, or LP and were cultured with Golgiplug (Pharmingen) in the presence or absence of N_{52-59} peptide for 5 hours at 37°C. Cells were washed, surface-stained with CD8α and CD11a, and permeabilized with PermWash (Pharmingen). After incubation with anti–IFN-γ, cells were washed and analyzed by flow cytometry. Plots shown are gated on CD8α+ lymphocytes; values are the mean percentages of IFN-γ+ or tetramer+ cells ± standard error within the CD8+ T cell population derived from at least four mice. (**B**) Twenty days after VSV infection, lymphocytes were incubated for 4 to 5 hours with ^{51}Cr-labeled untreated EL4 target cells (*27*) or target cells pulsed with N_{52-59} peptide. E:T ratio was 200:1 for all tissues. E:T values shown in plots are corrected for the number of tetramer+ cells in each population. Percentage of tetramer+ cells among total lymphocytes: spleen, 0.3%; LP, 1.0%; lung, 1.2%; liver, 1.0%. Data shown are derived from a single spleen (similar results were obtained using spleens from three other mice) and pools of liver, LP, or lung cells from two mice (an equivalent pool from two additional mice gave similar results). (**C**) As described in (B), except lymphocytes were isolated from mice primed with 10^6 PFU of VSV–New Jersey, rested >7 months, then infected with VSV-Indiana and rested an additional 224 days. E:T ratio was 300:1 for all tissues. E:T values shown in plots are corrected for the number of tetramer+ cells. Percentages of tetramer+ cells among total lymphocytes: spleen, 1.1%; LP, 0.5%; lung, 1.7%; liver, 1.2%. Data shown are derived from a single spleen and LP (similar results were obtained from these tissues from three other mice), a pool of liver cells from two mice (an equivalent pool from two additional mice gave similar results), and a pool of lung cells from four mice. Spontaneous ^{51}Cr release was <10% and specific lysis was <5% in the absence of peptide. (**D**) Comparison of lytic activity from primary and memory CD8 T cells. Cells from spleen (squares) or lung (arrowheads), from mice infected with VSV 7 days previously (open symbols) or secondarily 224 days previously (solid symbols), were tested against N_{52-59} peptide–coated ^{51}Cr-labeled EL4 target cells in a 5-hour assay.

Memory Extinction, Learning Anew, and Learning the New: Dissociations in the Molecular Machinery of Learning in Cortex

Diego E. Berman and Yadin Dudai*

The rat insular cortex (IC) subserves the memory of conditioned taste aversion (CTA), in which a taste is associated with malaise. When the conditioned taste is unfamiliar, formation of long-term CTA memory depends on muscarinic and β-adrenergic receptors, mitogen-activated protein kinase (MAPK), and protein synthesis. We show that extinction of CTA memory is also dependent on protein synthesis and β-adrenergic receptors in the IC, but independent of muscarinic receptors and MAPK. This resembles the molecular signature of the formation of long-term memory of CTA to a familiar taste. Thus, memory extinction shares molecular mechanisms with learning, but the mechanisms of learning anew differ from those of learning the new.

Experimental extinction is the decline in the frequency or intensity of a conditioned response following the withdrawal of reinforcement (1). It does not reflect forgetting due to the obliteration of the original engram, but rather "relearning," in which the new association of the conditioned stimulus with the absence of the original reinforcer comes to control behavior (2, 3). Only a few studies so far have addressed cellular mechanisms of experimental extinction (4). We approached the issue by analyzing the extinction of CTA. In CTA, the subject learns to associate a taste with delayed malaise (5, 6). In the rat, the formation of long-term CTA memory depends on multiple mechanisms, including protein synthesis, in the IC, which contains the gustatory cortex (7–9). The requirement for protein synthesis is a universal of long-term memory consolidation (10–14). If experimental extinction of CTA is indeed a relearning process that generates a long-term trace, it should be blocked by inhibition of protein synthesis in the IC during the retrieval session of the extinction protocol.

Rats were subjected to CTA training on an unfamiliar taste, saccharin (15), followed by repeated presentation of the conditioned taste in the absence of the malaise-inducing agent.

This led to the extinction of CTA (Fig. 1B, part a). However, when the protein synthesis inhibitor anisomycin was microinfused into the IC before the first retrieval test (16), 3 days after training, under conditions that inhibit >90% of protein synthesis for ~2 hours (7), extinction was blocked, to be resumed only after the subsequent extinction session (Fig. 1B, part b). A second application of anisomycin, before the subsequent extinction session, again blocked extinction (Fig. 1B, part c). Administration of anisomycin 30 min after retrieval had no effect (Fig. 2A). The transient inhibition of protein synthesis during the retrieval of CTA to saccharin had no deleterious effect on acquisition of CTA to another taste 4 days later (17). It could be argued that anisomycin did not attenuate extinction but rather reinstated the original aversion by functioning as a negative reinforcer in association with the taste [as in unconditioned stimulus reexposure (2)]. This, however, was ruled out. First, under the conditions used in this experiment, anisomycin in the IC does not serve as a negative reinforcer in CTA (7). Second, introduction of anisomycin into the IC after extinction has further proceeded did not reinstate the original memory (Fig. 2B). Inhibition of protein synthesis during or immediately after an extinction trial therefore blocks extinction. This resembles the dependence of consolidation of a newly acquired memory on protein synthesis (7, 10–14).

The formation of long-term CTA memory requires multiple neuromodulatory and signal-transduction mechanisms in the IC (8, 9, 18, 19). These involve cholinergic and β-adrenergic receptors, the MAPK ERK1-2 cascade, and the transcription factor Elk-1. If extinction is a learning process, does it require the same cellular machinery as the initial learning? When microinfused into the IC at concentrations that block long-term CTA memory (8, 9, 18, 19), the N-methyl-D-aspartate (NMDA) receptor antagonist D,L-2-amino-5-phosphonovaleric acid (APV), the muscarinic antagonist scopolamine, and the ERK-kinase inhibitor PD98059, had no effect on extinction of CTA (Fig. 3). In contrast, the β-adrenergic receptor blocker propranolol, which blocks long-term CTA memory (9), also blocked its extinction. Thus only a fraction of the molecular systems that subserve CTA acquisition is required for the learning process that is manifested in extinction. None of these systems is essential for retrieval (Table 1).

If extinction is indeed an instance of learning, why does it not share with the original learning the activation of the muscarinic recep-

Department of Neurobiology, The Weizmann Institute of Science, Rehovot 76100, Israel.

*To whom correspondence should be addressed at yadin.dudai@weizmann.ac.il

Table 1. Comparison of the contribution of identified molecular entities to the acquisition (with a novel or a familiar taste), retrieval and extinction of long-term CTA. Symbols: +, indispensable for the process; −, dispensable. NMDAR, the NMDA receptor; mAChR, the muscarinic acetylcholine receptor; β-AR, the β-adrenergic receptor. The compilation is based on the present work, as well as on data from (8, 9, 18, 19).

Agent	Long-term CTA			
	Acquisition		Retrieval	Extinction
	Novel	Familiar		
NMDAR	+	+	−	−
mAChR	+	−	−	−
β-AR	+	+	−	+
MAPK	+	−	−	−
Protein synthesis	+	+	−	+